# Fast and Efficient 4x4 Tchebichef Moment Image Compression

Nur Azman Abu[1], Siaw Lang Wong[2], Hidayah Rahmalan[3], Shahrin Sahib[4]
1- Senior Lecturer, Faculty of Information and Communication Technology, Universiti Teknikal Malaysia Melaka (UTeM),
Email: nura@utem.edu.my
2- Postgraduate Student, Faculty of Information and Communication Technology, Universiti Teknikal Malaysia Melaka (UTeM),
Email: wong.siawlang@gmail.com
3- Lecturer, Faculty of Information and Communication Technology, Universiti Teknikal Malaysia Melaka (UTeM),
Email: hidayah@utem.edu.my
4- Dean, Faculty of Information and Communication Technology, Universiti Teknikal Malaysia Melaka (UTeM),
Email: shahrinsahib@utem.edu.my

Received: March 2010 Revised: May 2010 Accepted: July 2010

**ABSTRACT:**
Orthogonal moment functions have long been used in image analysis. This paper proposes a novel approach based on 4x4 discrete orthogonal Tchebichef moment for fast and efficient image compression. The method incorporates a simplified mathematical framework technique using matrices as well as a block-wise reconstruction technique to eliminate possible occurrences of numerical instabilities at higher moment orders. Then the 4x4 Tchebichef Moment Transform and Discrete Cosine Transform have been compared. The results show that the 4x4 Tchebichef moment has significant advantages over the other technique in terms of its error reconstruction, average bit-length of Huffman codes and image quality. Moreover, Tchebichef moment provides a compact support to sub-block reconstruction for image compression. Tchebichef Moment Compression clearly performs potentially better for broader domains on real digital images and graphically generated images.

**KEYWORDS:** Image Coding, Tchebichef Moment Transforms, Orthogonal Moment Functions, JPEG Compression, Discrete Cosine Transform.

## 1. INTRODUCTION

Moment functions have been widely used in several computer vision and related image processing applications. For examples, they are used in image analysis [1], texture segmentation [2], multispectral texture [3], pattern recognition [4][5], image watermarking [6], monitoring crowds [7]-[9], image reconstruction [10][11] and image projection [12].

Image compression is the art or science of efficient coding of picture data with a target to decrease the number of bits required in performing an image [13]. The benefits of image compression are saving time, for image transmission and memory, for image storage.

A block-wise moment computation scheme which avoids numerical instabilities to yield a perfect reconstruction has been introduced in [14]. Therefore, it is feasible for moment functions to be used in image compression [15]-[17].

The discrete Tchebichef Moment Transform (TMT) is a transform method using Tchebichef polynomials [15][18], which has good energy compactness properties and works better for a certain class of images. Due to these advantages, this paper analyzes the reconstruction aspects on real and graphical images for compression. Using the JPEG Compression platform, 4x4 TMT has been used here instead of Discrete Cosine Transform (DCT). The Tchebichef Moment Compression that is developed here is meant for smaller computing device.

This paper is organized as follows: Section 2 and 3 describes the Tchebichef moment and Discrete Cosine Transform. The matrix implementation of moment equation is reviewed in Section 4. Section 5 presents the comparison between JPEG baseline coding and 4x4 Tchebichef Moment Compression. The advantage of using 4x4 Tchebichef moments compression is discussed in Section 6 and conclusion is given in Section 7.

## 2. TCHEBICHEF MOMENTS

Let $T_{mn}$ be Tchebichef moments based on a discrete orthogonal polynomial set $\{t_n(x)\}$ defined directly on the image space $[0, S–1]$, thus satisfying all the required analytical properties without any numerical approximation errors, $T_{mn}$ will be:

$$T_{mn} = \frac{1}{\rho(m,S)\rho(n,S)} \sum_{i=0}^{S-1}\sum_{j=0}^{S-1} t_m(i)t_n(j)f(i,j) \quad (1)$$

for $m$, $n$ = 0, 1, 2, …, $S$ –1.

For detail description of the properties of Tchebichef polynomials and the definitions of related terms such as the squared- norm $\rho()$, please refer to [11]. The Tchebichef orthogonal polynomials set $\{t_n(x)\}$ can be generated iteratively with initial conditions,

$$t_0(x)=1,$$

$$t_1(x)=\frac{2x+1-S}{S},$$

and the general Tchebichef orthogonal polynomial equation is represented as:

$$t_n(x)=\frac{(2n-1)\cdot t_1(x)\cdot t_{n-1}(x)-(n-1)\left(1-\frac{(n-1)^2}{S^2}\right)\cdot t_{n-2}(x)}{n} \quad (2)$$

for $n$ = 2, 3, …, $S$–1.

The first few discrete orthogonal Tchebichef polynomials are shown in Fig**.** 1. The above definition uses the following scale factor [18] for the polynomial of degree

$$\beta(n, S)= S^n \quad (3)$$

The set $\{t_n(x)\}$, has a squared-norm given by

$$\rho(n,S) = \sum_{i=0}^{S-1} \{t_i(x)\}^2$$

$$= \frac{S\cdot\left(1-\frac{1^2}{S^2}\right)\cdot\left(1-\frac{2^2}{S^2}\right)\cdot\left(1-\frac{3^2}{S^2}\right)\cdots\left(1-\frac{n^2}{S^2}\right)}{2n+1} \quad (4)$$

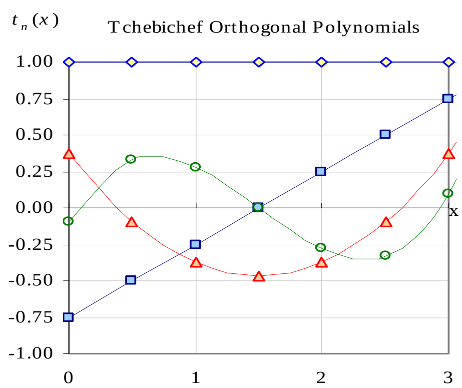


**Fig. 1**. The discrete orthogonal Tchebichef polynomials $t_n(x)$ for $n$ = 0, 1, 2 and 3.

Discrete orthogonal Tchebichef moment has its own advantage in image processing which has not been fully investigated. Since computer image data operates on integers, discrete orthogonal Tchebichef moment is suitable for computer image processing.

As shown in Fig. 1 the polynomial domain is discrete over natural numbers. Unlike continuous orthogonal transform, discrete orthogonal Tchebichef moment is capable of performing image reconstruction exactly without any numerical errors [14].

## 3. DISCRETE COSINE TRANSFORM

Since a comparison between the efficient techniques of Tchebichef Moment and Discrete Cosine Transform (DCT) is to be done, thus DCT is introduced in this section. DCT polynomial set $\{C_n(x)\}$ can be generated iteratively as follows,

$$C_0(x)=1,$$

$$C_1(x) = \cos\left(\frac{1\pi x}{4}\right),$$

$$C_2(x) = \cos\left(\frac{\pi x}{2}\right)\times\frac{1}{2},$$

$$C_3(x) = \cos\left(\frac{3\pi x}{4}\right)\times\frac{1}{3},$$

The general DCT polynomial equation is represented as:

$$C_n(x) = \cos\left(\frac{n\pi x}{S}\right)\times\frac{1}{n}, \quad (5)$$

for $n$ = 2, 3, …, $S$–1.

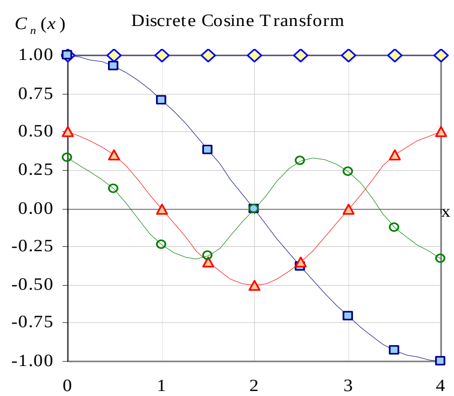


**Fig. 2**. The Discrete Cosine Transform polynomials $C_n(x)$ for $n$ = 0, 1, 2 and 3.

The first few DCT polynomials above are shown in Fig. 2 for visual purposes. According to [19], DCT is approaching a statistically optimal transform for highly correlated data with a first-order Markov model which is one of the most widely used transforms in digital signal processing. The kernel for the DCT is derived from the orthonormal Tchebichef polynomials, resulting from the following definition of *g'* [15]:

$$g'(x,u) = \lambda(u)\cos\left[\frac{\pi(2x+1)u}{2S}\right],$$

where

$$\lambda(u) = \begin{cases} \sqrt{\frac{1}{S}}, u = 0 \\ \sqrt{\frac{2}{S}}, u \neq 0 \end{cases}$$

DCT is a separable linear transform, which the two-dimensional transform is equivalent to a one-dimensional DCT performed along a single dimension followed by a one-dimensional DCT in the other dimension [20]. The definition of the two-dimensional DCT for an input image A and output image B is:

$$B_{pq} = \alpha_p \beta_q \sum_{m=0}^{M-1}\sum_{n=0}^{N-1} A_{mn} \cos\frac{\pi(2m+1)p}{2M} \cos\frac{\pi(2n+1)q}{2N},$$

Where

$$\alpha_p = \begin{cases} \sqrt{\frac{1}{M}}, p = 0 \\ \sqrt{\frac{2}{M}}, p > 0 \end{cases}, \qquad \alpha_q = \begin{cases} \sqrt{\frac{1}{N}}, q = 0 \\ \sqrt{\frac{2}{N}}, q > 0 \end{cases}$$

## 4. MATRIX IMPLEMENTATION OF MOMENT EQUATIONS

This section provides a compact representation of the moment equations and the inverse moment transform. The matrix based framework makes the problem description more amenable to mathematical programming languages such as MATLAB, MAPLE and the code is less prone to errors when processing large images.

In the following discussion, from (1) the moment set consists of all orders of moments with the values in range $0 < m, n < S$ of block size $0<S<N$, where the image size is $N$x$N$ pixels. The image matrix was subdivided into 4x4 pixels where the orthogonal moment on each block was computed independently. The block size $S$ is taken to be 4 and extendable to 8, 16 or 32. Based on the current 32-bit processor and word size, it is recommended to use $S$ = 16 for large industrial images in addition to the current popular $S$ = 8 as in JPEG.

For simplicity, consider the discrete orthogonal moment definition (1) above, and define a kernel matrix $\boldsymbol{K}_{(S\text{x}S)}$ as follows:

$$K = \begin{bmatrix} t_0(0) & t_1(0) & \cdots & t_{S-1}(0) \\ t_0(1) & t_1(1) & \cdots & t_{S-1}(1) \\ t_0(2) & t_1(2) & \cdots & t_{S-1}(2) \\ \vdots & \vdots & \ddots & \vdots \\ t_0(S-1) & t_1(S-1) & \cdots & t_{S-1}(S-1) \end{bmatrix} \quad (6)$$

Let the image block intensity matrix $\boldsymbol{F}_{(S\text{x}S)}$ with *f*() denoting the intensity values be

$$F = \begin{bmatrix} f(0,0) & f(0,1) & \cdots & f(0,S-1) \\ f(1,0) & f(1,1) & \cdots & f(1,S-1) \\ f(2,0) & f(2,1) & \cdots & f(2,S-1) \\ \vdots & \vdots & \ddots & \vdots \\ f(S-1,0) & f(S-1,1) & \cdots & f(S-1,S-1) \end{bmatrix} \quad (7)$$

The matrix $\boldsymbol{T}_{(S\text{x}S)}$ of moments defined according to (2) can now be formed as

$$\boldsymbol{T} = \boldsymbol{K}^{\mathrm{T}} \boldsymbol{F} \boldsymbol{K} \quad (8)$$

The inverse moment relation used to reconstruct the image block from the above moment set is now simply calculated by,

$$\boldsymbol{G} = \boldsymbol{K} \boldsymbol{T} \boldsymbol{K}^{\mathrm{T}} \quad (9)$$

where $\boldsymbol{G}_{(S\text{x}S)}$ denotes the matrix (image) of the reconstructed intensity values $g(i, j)$. The visual representation of the matrix (9) is given in Fig. 3. The resulting compressed image shall only consist of the moment coefficients.

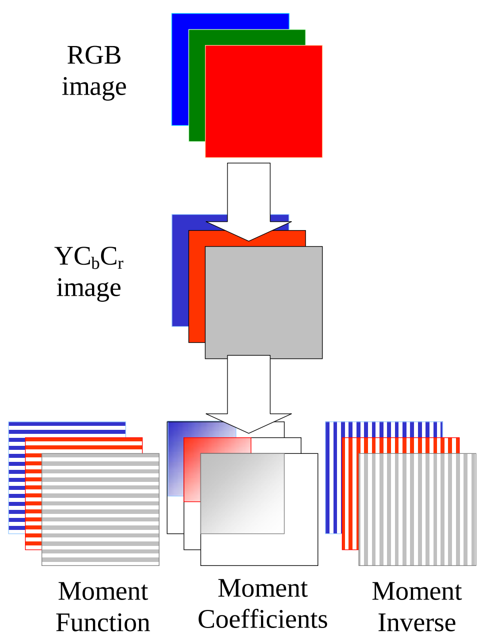


**Fig. 3**. The visual representation of the block matrices.

## 5. JPEG BASELINE CODING VERSUS 4X4 TCHEBICHEF MOMENT COMPRESSION

JPEG is an international compression standard which is designed to support a wide variety of applications for continuous-tone images. JPEG baseline is a simple lossy technique, which is a DCT-based method, has been commonly used today and is sufficient for a large number of applications. A good review of the JPEG compression standard may be found in [21].

Using the JPEG Compression platform, 4x4 TMT has been used here instead of DCT. Fig. 4 shows how the TMT performs on the 4x4 blocks of the image data. In order to achieve good compression performance, correlation between the color components is first reduced by converting the RGB color space into a décor-related color space, a RGB to $YC_bC_r$ conversion. RGB shall be separated into a luminance part (Y) and two chrominance parts ($C_b$ and $C_r$) as recommended by the JPEG standard.

To apply TMT, the image is divided into 4x4 blocks of pixels. The 4x4 blocks are processed from left-to-right and from top-to-bottom. After the transformation, two main issues occur, which are: the quantization process and the entropy coding.

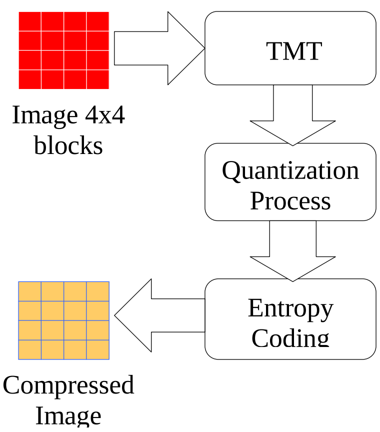


**Fig. 4**. Tchebichef Moment Compression consists of TMT instead of 2-dimensional DCT.

### 5.1. Quantization

For each layers, the moment coefficients shall be quantized separately. The quantization process has the key role in JPEG compression which removes the high frequencies present in the original image. This is done due to the fact that the eye is much more sensitive to lower spatial frequencies than to higher frequencies. This is done by dividing values at high indexes in the vector (the amplitudes of higher frequencies) with larger values than the values by which the amplitudes of lower frequencies are divided by.

The Standard JPEG luminance and chrominance quantization tables $Q_L$ and $Q_R$ are given below, respectively.

$$Q_L = \begin{bmatrix} 16 & 11 & 10 & 16 \\ 12 & 12 & 14 & 19 \\ 14 & 13 & 16 & 24 \\ 14 & 17 & 22 & 29 \end{bmatrix} \quad Q_R = \begin{bmatrix} 17 & 18 & 24 & 47 \\ 18 & 21 & 26 & 66 \\ 24 & 26 & 56 & 99 \\ 47 & 66 & 99 & 99 \end{bmatrix}$$

The 2-dimensional DCT performed on the 4x4 sub-blocks of the image data generates 4-bit gains. The quantization table for luminance starts with $2^4 = 16$. However, Tchebichef moment generates only 2-bit gains. The quantization tables for Tchebichef moment should start with $2^2 = 4$. The second author proposed the corresponding luminance and chrominance quantization tables $Q_{ML}$ and $Q_{MR}$ below for Tchebichef Moment Compression. These tables may be generated mathematically in a friendlier manner.

$$Q_{ML} = \begin{bmatrix} 4 & 6 & 8 & 16 \\ 6 & 8 & 16 & 32 \\ 8 & 16 & 32 & 64 \\ 16 & 32 & 64 & 128 \end{bmatrix} \quad Q_{MR} = \begin{bmatrix} 4 & 8 & 16 & 32 \\ 8 & 16 & 32 & 64 \\ 16 & 32 & 64 & 128 \\ 32 & 64 & 128 & 256 \end{bmatrix}$$

80 traditionally popular images have been selected and went through the basic image compression experimental validation. These images are categorized into 40 real images and 40 graphical images, respectively. All the images are raw RGB 3-layer images of size 512x512 pixels.

### 5.2. Entropy Huffman Coding

After the transformation and quantization over a 4x4 image sub-blocks, the new 4x4 sub-block shall be reordered in a zigzag scan into a linear array as shown in Fig. 5. The first coefficient is the DC component and the other 15 coefficients are AC component. Because the DC coefficient contains a lot of energy, it usually has much larger value than AC coefficients, and there is a very closer relation between the DC coefficients of adjacent blocks. Thus, DC coefficient is differentially encoded from consecutive 4x4 blocks rather than its true value.

| | | | |
|---|---|---|---|
| 0 | 1 | 5 | 6 |
| 2 | 4 | 7 | 12 |
| 3 | 8 | 11 | 13 |
| 9 | 10 | 14 | 15 |

**Fig. 5**. Zigzag reordering pattern.

The basic entropy coding is used here. It consists of the Huffman Coding as recommended in the JPEG standard. There are four Huffman tables; two for encoding DC coefficients and two for encoding AC coefficients. They are DC luminance, DC chrominance, AC luminance and AC chrominance tables. The Huffman tables used during the compression process are stored as header information in the compressed image file in order to uniquely decode the coefficients during the decompression process [22].

The average bit-length for Huffman codes between DCT and TMT for real and graphical set of images have been calculated. TMT requires approximately the same average bit-length as DCT as shown in Table 1 for real images and Table 2 for graphical images. This indicates that TMT has the same compression rate with DCT during encoding process.

**Table 1**. Average Bit Length for Huffman codes between DCT and TMT for real images

| Real Image | DCT | TMT | Diff. |
|---|---|---|---|
| DC Luminance | 4.1051 | 4.1382 | 0.0331 |
| DC Chrominance | 1.8351 | 1.8877 | 0.0526 |
| AC Luminance | 1.8425 | 1.8558 | 0.0133 |
| AC Chrominance | 1.0386 | 1.0439 | 0.0053 |

**Table 2**. Average Bit Length for Huffman codes between DCT and TMT for graphical images

| Graphical Image | DCT | TMT | Diff. |
|---|---|---|---|
| DC Luminance | 4.0425 | 4.0451 | 0.0026 |
| DC Chrominance | 2.8128 | 2.8703 | 0.0575 |
| AC Luminance | 1.9571 | 1.9913 | 0.0342 |
| AC Chrominance | 1.1657 | 1.1791 | 0.0134 |

### 5.3. Error Analysis

Calculating the energy compactness of a transform cannot be calculated directly, and instead is approximated by analyzing the reconstruction error of the transform. The full image reconstruction error is calculated by the difference between the input and output images for each transform. Thus, it can be defined as

$$E(S) = \frac{1}{3MN} \sum_{i=0}^{M-1} \sum_{j=0}^{N-1} \sum_{k=0}^{2} \left| g(i,j,k) - f(i,j,k) \right| \quad (10)$$

where the third index in the intensity value refers to the three color RGB layers.

Apart from that, some other measurements are required to represent the reconstruction accuracy. Mean Squared Error (MSE) calculates the average of the square of the error. The error is the amount by which the estimator differs from the quantity to be estimated. The difference occurs because of randomness or because the estimator does not account for information that could produce a more accurate estimate. The MSE is defined as

$$MSE = \sum_{i=0}^{M-1} \sum_{j=0}^{N-1} \sum_{k=0}^{R-1} \left\| I(i,j,k) - K(i,j,k) \right\|^2 \quad (11)$$

which for two $M \times N \times R$ color images $I$ and $K$ where one of the images is considered a noisy approximation of the other.

The standard Peak-Signal-to-Noise Ratio (PSNR) is used as well. It is most commonly used as a measure of quality of reconstruction of compression. A higher PSNR would indicate that the reconstruction is of higher quality.

$$PSNR = 20 \cdot \log_{10}\left( \frac{MAX_I}{\sqrt{MSE}} \right) = 10 \cdot \log_{10}\left( \frac{255^2}{\sqrt{MSE}} \right)$$

$MAX_I$ is the maximum possible pixel value of the image. In this case, when the pixels are represented using 8 bits per sample, its value will be 255.

Moreover, Average Difference (AD) and Maximum Difference (MD) are also been calculated for the comparison. AD is to measure the average difference that occurred between original image and reconstructed image, while MD is to measure the maximum difference that occurred between the original image and reconstructed image. The formulas are defined as below

$$AD = \sum_{i=0}^{M-1} \sum_{j=0}^{N-1} \sum_{k=0}^{R-1} \left\| I(i,j,k) \right\| \quad (12)$$

$$MD = \max_{0 \le i < M} \{ \max_{0 \le j < N} \{ \max_{0 \le k < R} \{ \left| I(i,j,k) \right| \} \} \} \quad (13)$$

On average, TMT performs consistently better than DCT in quality image reconstruction for real and graphical images as shown in Table 3 and Table 4 respectively. The results show that TMT produces smaller reconstruction errors and higher PSNR. This indicates that the TMT encodes better quality for compressed images.

**Table 3**. Average error score between DCT and TMT for 40 real images

| Real Image | DCT | TMT | Diff. |
|---|---|---|---|
| Full Error | 4.2852 | 4.0167 | -0.2685 |
| MSE | 36.3798 | 32.7326 | -3.6472 |
| PSNR | 33.4683 | 33.7317 | 0.2634 |
| AD | -0.0241 | -0.0655 | -0.0414 |
| MD | 55.8250 | 45.9500 | -9.8750 |

**Table 4**. Average error score between DCT and TMT for 40 graphical images

| Graphical Image | DCT | TMT | Diff. |
|---|---|---|---|
| Full Error | 3.8875 | 3.2319 | -0.6556 |
| MSE | 37.7305 | 28.1534 | -9.5771 |
| PSNR | 34.0483 | 34.8735 | 0.8252 |
| AD | -0.0558 | -0.1102 | -0.0544 |
| MD | 66.7250 | 50.8750 | -15.8500 |

The Tchebichef moment performs better in this case especially for graphical images as expected. This has been due to the linear first order Tchebichef polynomial

$$t_1(x) = \frac{2x+1-S}{S}.$$

Moreover, from the results shown in tables [23] below, it is indicated that TMT has the same compression rate with DCT during the encoding process. 4x4 image block coding is more compact than 8x8 in terms of lossless compression such as Huffman codes with the same image reconstruction quality as numerically shown in Table 5 and Table 6.

**Table 5**. Average bit length of Huffman codes between DCT and TMT for real images

| Real Image | 4 x 4 | | 8 x 8 | |
|---|---|---|---|---|
| | DCT | TMT | DCT | TMT |
| DC Luminance | 4.1051 | 4.1382 | 5.7730 | 4.7660 |
| DC Chrominance | 1.8351 | 1.8877 | 2.7635 | 2.0237 |
| AC Luminance | 1.8425 | 1.8558 | 2.8395 | 1.7680 |
| AC Chrominance | 1.0386 | 1.0439 | 2.9970 | 2.3589 |

**Table 6**. Average bit length of Huffman codes between DCT and TMT for graphical images

| Graphical Image | 4 x 4 | | 8 x 8 | |
|---|---|---|---|---|
| | DCT | TMT | DCT | TMT |
| DC Luminance | 4.0425 | 4.0451 | 5.5088 | 4.9000 |
| DC Chrominance | 2.8128 | 2.8703 | 4.2354 | 3.2357 |
| AC Luminance | 1.9571 | 1.9913 | 2.1093 | 1.2124 |
| AC Chrominance | 1.1657 | 1.1791 | 2.4756 | 2.0027 |

Fig. 6 shows the 400% compressed image of Baboon, zoomed to the right eye, using DCT and TMT methods, along with the original image. Based on Fig. 6b, DCT gives a smoother output whereas the output of TMT projected sharper and closer in consider to the original image in Fig. 6c. In refer to numerical analysis; the reconstruction error for Baboon right eye via DCT method is 6.9681 while the reconstruction error for Baboon right eye via TMT method is 6.7007. This indicates that the TMT encodes better quality for Baboon compressed image. Nonetheless, similar results have been observed in image projection [24] as well.

Even though in real life it is ideally rare to find straight lines, in reality there are many near straight curves within significant portions of an image especially among graphical images. Thus, Tchebichef moment converges faster than DCT via fewer low frequency coefficients.

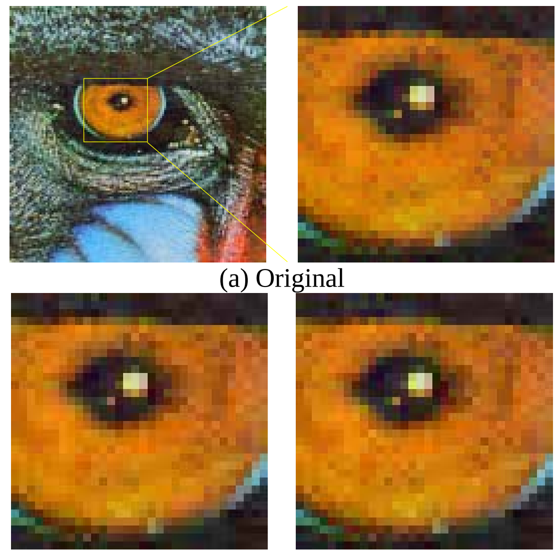

(a) Original

(b) DCT (c) TMT

**Fig. 6**. Comparison of compressed images from (a) Original image using (b) DCT and (c) TMT methods.

### 5.4. Frequency Distribution

In this section, a discussion on the frequency distribution of the transform coefficients on forty real images via TMT transformation technique is presented. Frequency distribution is a summary of the values obtained and the frequencies which these values have occurred.

Fig. 7(a)-(d) shows the frequency distribution of DC coefficients for luminance, DC coefficients for chrominance, AC coefficients for luminance and AC coefficients for chrominance via the Tchebichef Moment Transform on forty real images, respectively. The frequency decreases exponentially from the center coefficients of zero. This characteristic can be exploited in the cause of generating the lossless codes of the TMT coefficients for compression.

## 6. THE ADVANTAGES OF 4X4 TCHEBICHEF MOMENT COMPRESSION

Image is becoming an important element in daily life. Computing devices is getting smaller and affordable. Current popular small computing device such as mobile phones require a lot of image transmission and processing. It is always essential to have efficient image compression technique which is scalable and portable to smaller computing device such as personal digital assistance and mobile phones.

The Tchebichef Moment Compression that has been developed in this paper is meant for smaller computing devices. The efficiency of Tchebichef Moment Compression is much higher than of DCT in terms of the compression performance. As proposed in [25], a new fast 4x4 forward Discrete Tchebichef Transform algorithm can also be used as the base core for TMT computation using recursive reduction of polynomial orders. The experimental results have shown that the proposed algorithm reduces the time taken to transform images of different size efficiently.

In addition, this Tchebichef Moment Compression has the potential to be applicable not only for continuous natural digital images but also for generic artificial images generated by graphical software. Concurrently, it has lower computational complexity since it does not require special algorithms for DCT [26]. This advantage makes it simpler and a more feasible software implementation for new software and hardware developers.

The Tchebichef Transform has the additional advantage of requiring the evaluation of only algebraic expressions, whereas certain implementations of DCT require lookup tables for computing trigonometric functions [25]. Two important characteristics of Tchebichef moments are:

i. a discrete domain of definition which matches exactly with the image coordinate space, and
ii. absence of numerical approximation terms allows a more accurate representation of image features than otherwise possible using conventional moments [11].

## 7. CONCLUSION

This paper proposes the TMT as a possible alternative to DCT for applications in image compression and reconstruction. Discrete orthogonal moment using Tchebichef polynomials as basic functions were initially introduced as a feature descriptor that eliminates many problems associated with geometric as well as continuous moment functions like Zernike and Legendre moments.

Images can also be exactly reconstructed from a complete set of Tchebichef Discrete Orthogonal Moments. This paper also proposes a simplified matrix-based implementation. At the same time, the experimental results show that the Tchebichef moment provides better quality with the same compression rate on small computing devices via 4x4 sub-block reconstruction compression. This is evidenced by obtaining a smaller reconstruction error and similar average bit-length of Huffman codes. The Tchebichef Moment Compression has the potential to perform better for broader domains on real digital images and graphically generated images.

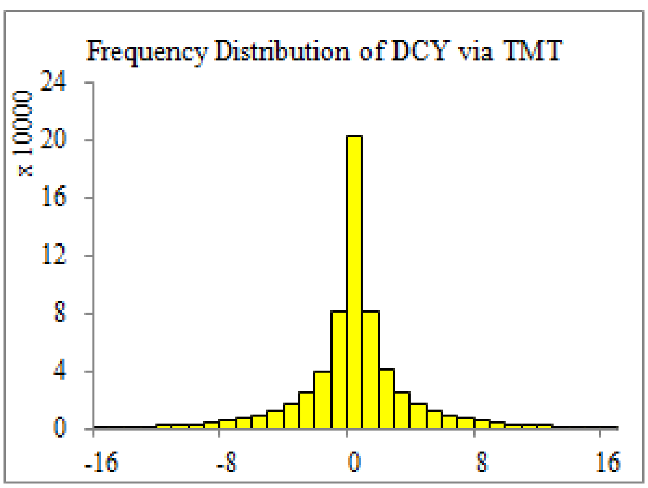

(a) The frequency distribution of DC coefficients for luminance.

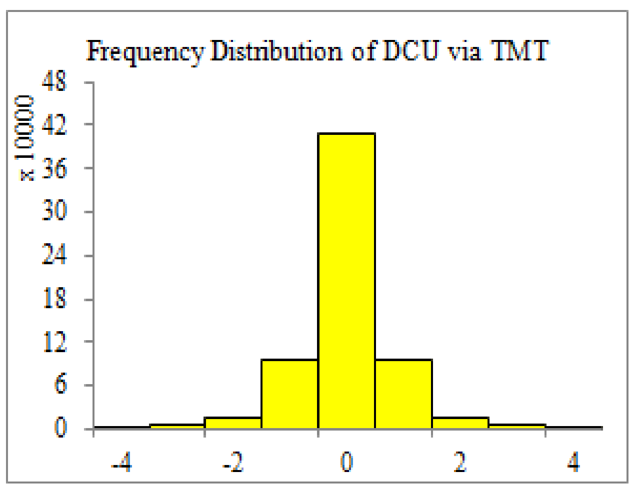

(b) The frequency distribution of DC coefficients for chrominance.

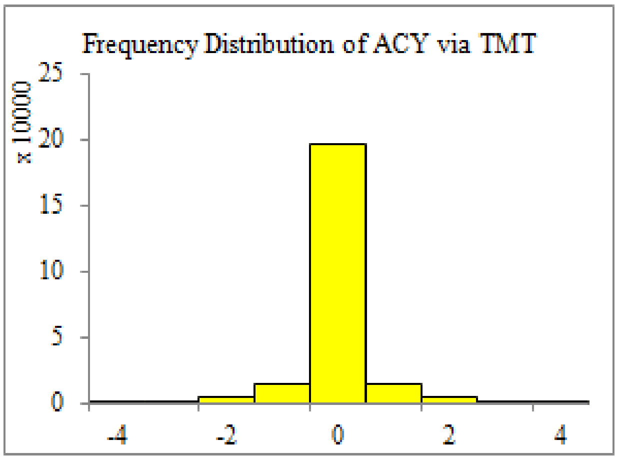


(c) The frequency distribution of AC coefficients for luminance.

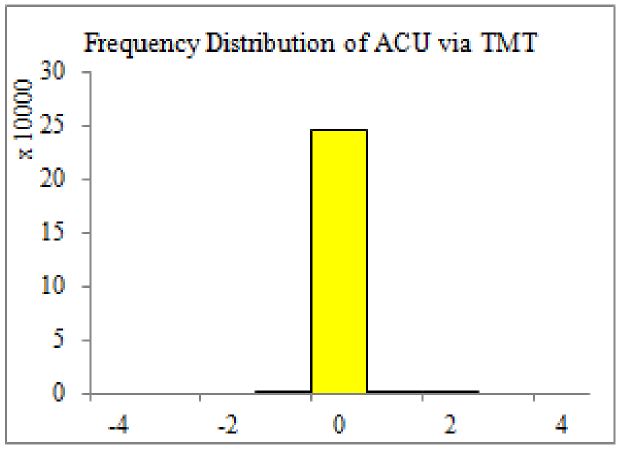


(d) The frequency distribution of AC coefficients for chrominance.

**Fig. 7**. The preliminary analysis for frequency distribution via Tchebichef Moment Transform on forty real images.

## 8. ACKNOWLEDGMENT

This research is financially supported by Fundamental Research Grant Scheme FRGS/2007/FTMK(3)-F0050 from Ministry of Higher Education, Malaysia.

## REFERENCES

[1] Cho-Huak Teh and Roland T. Chin; **"On Image Analysis by the Methods of Moments"**, *IEEE Transactions on Pattern Analysis Machine Intelligence*, Vol. 10, No. 4, pp. 496-513, ISSN 0162-8828, (1988)

[2] Tuceryan M., **"Moment Based Texture Segmentation"**, *Pattern Recognition Letters*, Vol. 15, pp. 659-668, (July 1994)

[3] Wang L. and Healey G.; **"Using Zernike Moments for the Illumination and Geometry Invariant Classification of Multispectral Texture"**, *IEEE Transactions on Image Processing*, Vol. 7, pp. 196-203, (1998)

[4] Shutler J.D.; **"Velocity Moments for Holistic Shape Description of Temporal Features"**, *PhD thesis, Department Electronic and Computer Science, University of Southampton*, (2001)

[5] Zhu Hongqing, Shu Huazhong, Xia Ting, Luo Limin, and Coatrieux Jean Louis; **"Translation and scale invariants of Tchebichef moments"**, *Pattern Recognition*, Vol. 40, No. 9, pp. 2530-2542, ISSN 0031-3203, (2007)

[6] Li Zhang, Qian Gong bin, Xiao Wei wei, and Ji Zhen; **"Geometric Invariant Blind Image Watermarking by Invariant Tchebichef Moments"**, *Optics Express Journal*, Vol. 15, pp. 2251-2261, (2007)

[7] Rahmalan H., Nixon M.S. and Carter J.N.; **"On Crowd Density Estimation for Surveillance"**, Proceedings of International Conference on Crime Detection and Prevention, London UK, (13-14 June 2006)

[8] Rahmalan H., Suryana N. and Abu N.A.; **"A General Approach for Measuring Crowd Movement"**, *Malaysian Technical Universities Conference and Exhibition on Engineering and Technology (MUCEET2009)*, pp. 98-103, Kuantan, Pahang, (20-22 June 2009)

[9] H. Rahmalan; **"Detecting Crowd Movement Using Moment Invariants"**, *International Conference on Image Processing, Computer Vision and Pattern Recognition IPCV'09*, Las Vegas, Nevada, (13-16 July 2009)

[10] Mukundan R.; **"Improving Image Reconstruction Accuracy Using Discrete Orthonormal Moments"**, *Proceedings of International Conference On Imaging Systems, Science and Technology*, pp. 287-293, (June 2003)

[11] Mukundan R.; **"Some Computational Aspects of Discrete Orthonormal Moments"**, *IEEE Transactions on Image Processing*, Vol. 13, No. 8, pp. 1055-1059, (Aug. 2004)

[12] Abu Nur Azman, Lang Wong Siaw and Sahib Shahrin; **"Image Projection Over The Edge"**, International Conference on Industrial and Intelligent Information (ICIII 2010), Proceedings 2nd International Conference on Computer and Network Technology (ICCNT 2010), pp. 344-348, Bangkok, Thailand, 23–25 April 2010)

[13] Rabbani M. and Jones P.W.; **Digital Image Compression Techniques (SPIE Press Book)**, Vol. TT07, ISBN 9780819406484, (1991)

[14] Abu Nur Azman, Suryana Nanna and Mukundan R.; **"Perfect Image Reconstruction Using Discrete Orthogonal Moments"**, *Proceedings of The 4th IASTED International Conference on Visualization, Imaging, and Image Processing (VIIP2004)*, pp. 903-907, Marbella, SPAIN, (6-8 September 2004)

[15] Mukundan R. and Hunt O.; **"A Comparison of Discrete Orthogonal Basis Functions for Image Compression"**, *Proceedings Conference on Image and Vision Computing New Zealand (IVCNZ 2004)*, pp. 53-58, (2004)

[16] Lang Wong Siaw, Abu Nur Azman, Rahmalan Hidayah; **"Fast 4x4 Tchebichef Moment Image Compression"**, *Proceedings International Conference*

*of Soft Computing and Pattern Recognition (SoCPaR) 2009*, pp. 295−300, Melaka, Malaysia, (4-7 December 2009)

[17] Abu Nur Azman, Lang Wong Siaw, Suryana Nanna and Mukundan Ramakrishnan; **"An Efficient Compact Tchebichef moment for Image Compression"**, 10th International Conference on Information Science, Signal Processing and their applications (ISSPA2010), pp.448-451, Kuala Lumpur, (10–13 May 2010)

[18] Mukundan R., Ong S.H. and Lee P.A.; **"Image Analysis by Tchebichef Moments"**, *IEEE Transactions on Image Processing*, Vol. 10, No. 9, pp. 1357–1364, (September 2001)

[19] Ahmed N., Neterajan T. and Rao K.R.; **"Discrete Cosine Transform"**, *IEEE Transactions on Computers*, Vol. 23, pp. 90-93, (January 1974)

[20] Anil K. Jain; **Fundamentals of Digital Image Processing**, *Prentice Hall*, pp. 172, (2006)

[21] Wallace Gregory K.; **"The JPEG Still Picture Compression Standard"**, *Communication of the ACM*, Vol. 34, No. 4, pp. 31-44, (April 1991)

[22] Acharya Tinku and Ajoy K. Ray; **Image Processing: Principles and Applications**, *John Wiley*, pp. 365, (2005)

[23] Rahmalan Hidayah, Abu Nur Azman and Wong Siaw Lang; **"Using Tchebichef Moment for Fast and Efficient Image Compression"**, *Journal of Pattern Recognition and Image Analysis*, No. 4, to be published, (2010)

[24] Abu Nur Azman, Wong Siaw Lang and Sahib Shahrin; **"Image Super-Resolution via Discrete Tchebichef Moment"**, *Proceedings of International Conference on Computer Technology and Development (ICCTD 2009)*, Vol. 2, pp. 315–319, Kota Kinabalu, Malaysia, (13–15 November 2009)

[25] Nakagaki Kiyoyuki and Mukundan Ramakrishnan; **"A Fast 4x4 Forward Discrete Tchebichef Transform Algorithm"**, *IEEE Signal Processing Letters*, Vol. 14, No. 10, pp. 684-687, (October 2007)

[26] Christopoulos C.A., Philips W., Skodras A.N. and Cornelis J.; **"Discrete Cosine Transform Coding of Images"**, *Proceedings of International Conference on DSP and CAES*, Vol. I, pp. 164-169, Nicosia, Cyprus, (14-16 July 1993)